Base-controlled product switch in the ruthenium-catalyzed protodecarbonylation of phthalimides: a mechanistic study

Massimo Christian d'Alterio, Yu-Chao Yuan, Christian Bruneau, Giovanni Talarico, Rafael Gramage-Doria, Albert Poater

Catalysis Science & Technology

Accepted Manuscript

This article can be cited before page numbers have been issued, to do this please use: M. C. D'Alterio, Y. Yuan, C. Bruneau, G. Talarico, R. Gramage-Doria and A. Poater, *Catal. Sci. Technol.*, 2019, DOI: 10.1039/C9CY02047K.

ROYAL SOCIETY OF CHEMISTRY

rsc.li/catalysis

ARTICLE Journal Name

DOI: 10.1039/C9CY02047K

Base-controlled, product switch in the ruthenium-catalyzed protodecarbonylation of phthalimides: a mechanistic study

Received 00th January 20xx,
Accepted 00th January 20xx

DOI: 10.1039/x0xx00000x

Massimo Christian d'Alterio,[a,b] Yu-Chao Yuan,[c] Christian Bruneau,[c] Giovanni Talarico,[b] Rafael Gramage-Doria,*[c] Albert Poater*[a]

The whole reaction mechanism of the ruthenium-catalyzed protodecarbonylation of N-substituted phthalimides into secondary amides was unravelled by a combined experimental and theoretical study. The chemoselectivity of the reaction, which is catalyzed by *para*-cymene coordinated Ru(II) species all over the catalytic cycle, is exclusively controlled by the unique roles of the bases. Whereas in the presence of K_2CO_3 or KOH at high temperatures the same product (benzamide) is mainly formed, whereas at low temperatures KOH led to an unexpected side-product (phthalamic acid) and no reactivity was observed with K_2CO_3. The non-covalent interactions between the potassium cations and the different carbonyl groups in the molecules are key to provide a thermodynamically favourable pathway with energetically accessible transition states. The unexpected formation of carbon dioxide (CO_2) in the course of the reaction originates from the phthalimide substrate and the base K_2CO_3 in two different elementary steps, respectively.

Introduction

Over the past decades, homogeneous catalysis plays a pivotal role to cover the demands of our society.[1] For instance, the synthesis of many daily life chemicals (drugs, pesticides, OLED materials, commodities, polymers, etc.) comprise at least one step involving transition metal catalysed transformation and many of these reactions nowadays are being conducted at the multiton scale (i.e. the rhodium-catalyzed hydroformylation of alkenes).[2] Consequently, the fundamental understanding of the metal reactivity and the discovery of new chemical reactions are extremely appealing in view of generating sustainable and environmentally benign processes in academic and industrial laboratories.

Well-defined, transition metal catalysts derived from platinum, rhodium, iridium and palladium are, by far, the most widely used for fine chemical synthesis due to their versatility and ability to reach multiple oxidation states and multiple coordination geometries that can affect the reactivity of given substrates.[3] However, these metals are extremely expensive, very scarce on the Earth's crust and their related complexes are in general unstable towards air and moisture.[3] It seems convenient then, to turn the attention to more abundant, affordable and stable metal complexes. As such, ruthenium seems promising since it displays a large number of oxidation states (from +8 to -2) and coordination geometries comparable to most of the precious metals, which makes this metal interesting to replace the less abundant ones.[4] In addition, the reactivity of ruthenium complexes for fine chemical synthesis has been well-established during the last decades.[4] The most relevant breakthroughs in this context are (1) the asymmetric hydrogenation of ketones into chiral alcohols with Ru-BINAP-diamine complexes by Noyori,[5] (2) the olefin metathesis reaction with $RuCl_2(PCy_3)_2(CHPh)$ as pre-catalyst by Grubbs,[6] and (3) the C-H bond functionalization of aryl moieties with $RuH_2(CO)(PPh_3)_3$ as pre-catalyst by Murai using ketones as directing groups.[7]

Aiming at discovering new chemical reactivity at ruthenium, some us have recently reported a general and high functional group tolerant protodecarbonylation of *N*-substituted phthalimides into amides using $[RuCl_2(p\text{-cymene})]_2$ as pre-catalyst in the presence of K_2CO_3 and water at high temperatures (Scheme 1).[8] Herein, we show detailed control experiments together with theoretical calculations at the DFT level to identify the mechanism operating in this ruthenium-catalyzed reaction, in particular, regarding the five-membered ring-opening step.[9] Key for the success of the reaction is the manifold roles played by the base. In particular, the non-covalent interactions between potassium cations and carbonyl groups as well as an unexpected intramolecular nucleophilic attack prior to the release of CO_2 have been identified. An interesting switch of product selectivity is observed when using KOH instead of K_2CO_3 as the base. It is relevant to note that the formal opposite reaction, namely the CO-carbonylation of amides into phthalimides catalysed by ruthenium and rhodium has been reported by Chatani;[10] and Rovis, respectively.[11] Recently, Goossen, Hartwig and Zhao, Hong, Baidya, and Shi, independently, have also reported appealing ruthenium-catalyzed decarboxylative reactions with structurally-related benzoic acid derivatives,[12] apart from the homologous work with nickel[13] and palladium.[14]

[a] Institut de Quimica Computacional i Catalisi and Departament de Quimica, Universitat de Girona, c/ Mª Aurelia Capmany 69, 17003 Girona, Catalunya, Spain. E-mail: albert.poater@udg.edu
[b] Dipartimento di Scienze Chimiche, Universita di Napoli Federico II, Via Cintia, I-80126 Napoli, Italy.
[c] Univ Rennes, CNRS, ISCR-UMR6226, F-35000 Rennes, France. E-mail: rafael.gramage-doria@univ-rennes1.fr

Electronic Supplementary Information (ESI) available: NMR data, all cartesian XYZ coordinates, and energies of all species. See DOI: 10.1039/x0xx00000x

View Article Online
DOI: 10.1039/C9CY02017K

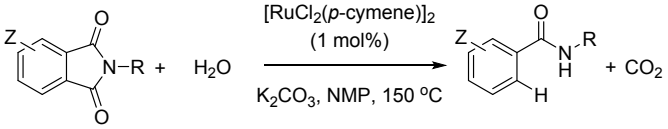

Scheme 1. Ruthenium-catalyzed protodecarbonylation of phthalimides whose mechanism is studied in this contribution. [NMP = *N*-methyl-2-pyrrolidone; R = alkyl, benzyl, aryl; Z = F, Cl, NO_2, Me; tolerant to -CN, -OMe, $-CF_3$, -Br, -I, -C(O)Me, $-CO_2Et$, pyridine, quinoline, thiophene]

Results and discussion

Catalytic experiments

The optimal reaction conditions previously developed consisted in $[RuCl_2(p\text{-cymene})]_2$ (1 mol%), 1.5 equivalent of water and 3 equivalents of K_2CO_3 at 150 °C during 6 hours.[8] Under these reaction conditions, *N*-methylphthalimide (**1**) fully reacted leading to *N*-methylbenzamide (**2**) in almost quantitative yield (Table 1, entry 1). Previous, preliminary mechanistic investigations indicated that CO_2 was formed in the course of the reaction and water served as the source of protons according to GC gas phase analysis and deuteration experiments, respectively.[8] A classical hydrogenation pathway was unlikely as the reaction did not occur in the presence of H_2 gas; and a slight excess of K_2CO_3 and water was required for the success of the transformation.[8] In addition, radical trapping experiments and mercury tests suggested an homogeneous pathway involving no formation of radicals.[8]

With this background, we performed a number of experiments with different ruthenium complexes as pre-catalysts in view of understanding which ligands lead to catalytically productive ruthenium species. K_2CO_3 and KOH bases were evaluated at different temperatures as shown in Table 1. The same catalytic outcome was observed with 2 mol% of $[Ru(p\text{-cymene})(MesCO_2)_2]$ (Mes = 2-mesityl) as the pre-catalyst (Table 1, entry 2),[15] whereas a poor conversion of 30% was observed with 2 mol% of the *para*-cymene-free $[Ru(NC^tBu)_6(BF_4)_2]$ complex and no formation of the expected product **2** (Table 1, entry 3).[16] These data strongly suggested that the catalytically active metal complex involved chloride-free, monomeric *para*-cymene-coordinated ruthenium(II) species.

For comparison purposes, we performed a reaction with KOH as the base instead of K_2CO_3 as we reasoned that the anion of the base (hydroxyl *versus* carbonate) could influence the catalysis to some extent. At 150 °C with 1 mol% of $[RuCl_2(p\text{-cymene})]_2$, full conversion of **1** was observed with the unexpected side-formation of *N*-methylphthalamic acid (**3**) together with the benzamide **2** as the products (Table 1, entry 4). Interestingly, **3** became the major product of the reaction when decreasing the temperature to 100 °C (Table 1, entry 5) and at room temperature it was exclusively formed with full conversion of **1** (Table 1, entry 6). It is important to note that metal-free, base-mediated five-membered ring-opening of *N*-substituted phthalimides are known to occur only at high temperatures,[17] which further supports that the formation of **3** at room temperature using KOH is indeed catalysed by ruthenium species. In stark contrast, using K_2CO_3 as the base at room temperature led to no conversion of starting material **1** (Table 1, entry 7). The starting material was recovered unreacted when the reaction was performed without base regardless of the temperature (Table 1, entries 8-9).[8]

Table 1. Evaluation of ligand, base, and temperature in the ruthenium-catalyzed protodecarbonylation of phthalimide **1**.[a]

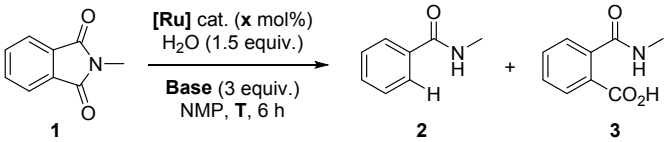

Entry	[Ru] (x mol%)	Base	T (°C)	**1** : **2** : **3**[b]
1	$[RuCl_2(p\text{-cymene})]_2$ (1)	K_2CO_3	150	0 : 100 : 0
2	$[Ru(p\text{-cymene})(MesCO_2)_2]$ (2)	K_2CO_3	150	0 : 100 : 0
3	$[Ru(NC^tBu)_6(BF_4)_2]$ (2)	K_2CO_3	150	70 : 0 : 0[c]
4	$[RuCl_2(p\text{-cymene})]_2$ (1)	KOH	150	0 : 72 : 28
5	$[RuCl_2(p\text{-cymene})]_2$ (1)	KOH	100	0 : 10 : 90
6	$[RuCl_2(p\text{-cymene})]_2$ (1)	KOH	25	0 : 0 : 100
7	$[RuCl_2(p\text{-cymene})]_2$ (1)	K_2CO_3	25	100 : 0 : 0
8	$[RuCl_2(p\text{-cymene})]_2$ (1)	-	25	100 : 0 : 0
9	$[RuCl_2(p\text{-cymene})]_2$ (1)	-	100	100 : 0 : 0

[a]Reaction conditions: **1** (0.4 mmol), H_2O (0.6 mmol), base (1.2 mmol), NMP (2 mL), Argon. [b]Determined by ^1H NMR spectroscopy using 1,3,5-trimethoxybenzene as internal standard and by GC-MS analysis. [c]Unknown by-products are formed.

DFT calculations

Taking into account all the previous experimental data and the difficulty to isolate any potential ruthenium intermediates during the catalysis,[8] theoretical calculations at the DFT level were carried out to gain a better understanding of the origin of the chemoselectivity observed by swapping the base in the ruthenium-catalyzed protodecarbonylation of phthalimides (Figure 1).[18]

First, the catalytic cycle was studied for the case where K_2CO_3 as the base is employed, which selectively leads to benzamide **2** at 150 °C (Figure 1A). The initial catalytically active species for the calculations was rationalized to be a cationic 16 electron Ru(II) complex with one μ^6-coordinated *para*-cymene ligand and one κ^2-coordinated carbonate ligand with a vacant site at ruthenium (**CAT**, Figure 1A). Such hypothesis is further supported by the findings from Demerseman and co-workers who reported that $[Ru(p\text{-cymene})Cl_2(PR_3)]$ (R= Me, Cy, Ph) reacted with K_2CO_3 in a polar solvent (i.e. acetone) leading to $[Ru(p\text{-cymene})(\kappa^2\text{-}O_2CO)(PR_3)]$

View Article Online
DOI: 10.1039/C9CY02047K

species.[19] In addition, we verified that the reaction of $[RuCl_2(p\text{-cymene})]_2$ with K_2CO_3 releasing KCl and forming $[Ru(p\text{-cymene})(\kappa^2\text{-}O_2COK)]^+$ (**CAT**) is highly exergonic with ΔG = -40.1 kcal/mol (see ESI for details).

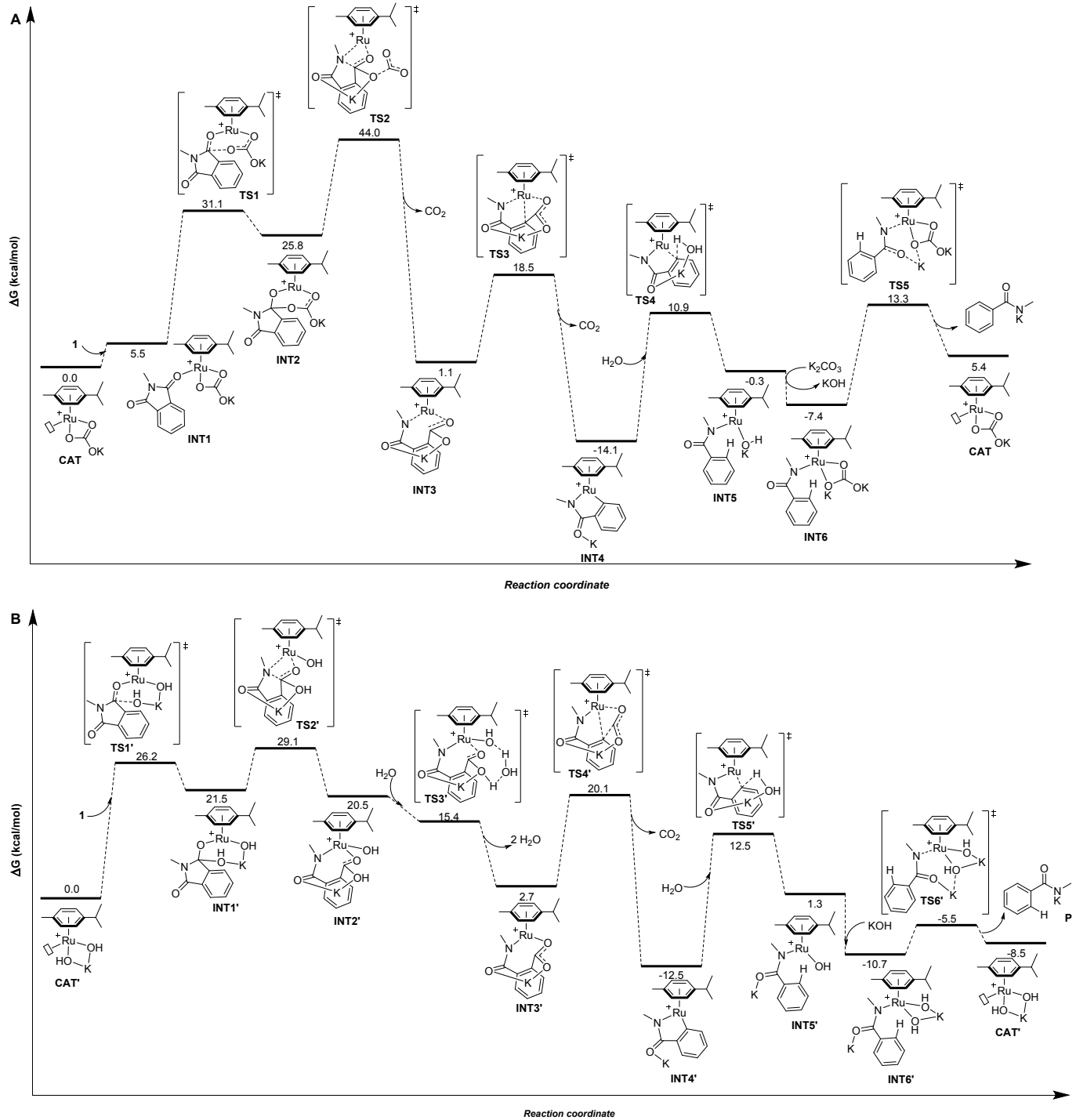

Figure 1. (**A**) Computed, minimum free energy reaction profile (in kcal/mol) for the ruthenium-catalyzed protodecarbonylation of **1** assisted by K_2CO_3, and (**B**) computed, minimum free energy reaction profile (in kcal/mol) for the ruthenium-catalyzed protodecarbonylation of **1** assisted by KOH.

In the intermediate **INT2**, the hybridization of one carbon atom switches from sp^2 in **INT1** to sp^3 in **INT2** with a subsequent elongation of the C-N bond by 0.06 Å ($d_{C\text{-}N}$ = 1.39 Å in **INT1** *versus* $d_{C\text{-}N}$ = 1.45 Å in **INT2**). Next, the simultaneous five-membered ring-opening of **1** and the decarboxylation from the carbonate fragment occurs *via* **TS2** (Figure 2A) giving rise to intermediate **INT3** (Figure 1A).

TS2 appears to be the rate determining step of the catalytic cycle with an energetic cost of 44.0 kcal/mol with respect to **CAT** (Figure 1A). The calculated energetic barrier is in full agreement with the experimental reaction temperature of 150 °C required for the success of the catalysis. Despite the latter energetically-demanding step *via* **TS2**, the previous intramolecular nucleophilic attack defined by **TS1** is crucial in kinetic terms as well, since the weakening of the C-N bond in **INT2** ($d_{C\text{-}N}$ = 1.45 Å, *vide supra*) makes the former substrate ready for the ring-opening (Figure 1A). Indeed, for comparison purposes, we modelled the transition state (TS) of the five-membered ring-opening of **1** without the previous nucleophilic attack. In this case, the substrate **1** coordinates to ruthenium *via* the nitrogen atom and a carbon atom belonging to the carbonyl group (Figure 2B) with an energetic barrier that goes up to 75.1 kcal/mol with respect to **CAT** in order to form the intermediate **INT3**. From intermediate **INT3**, a decarboxylation occurs within the substrate *via* **TS3** with an energy barrier of 17.4 kcal/mol with respect to **INT3**, affording the very stable five-membered ruthenacycle **INT4** (Figure 1A). The high stability of **INT4** is largely ascribed to the formation of the new Ru-C(aryl) bond. The next concerted **TS4**, with an energy barrier of 25.0 kcal/mol, requires the participation of one molecule of H_2O (Figure 1A). More precisely, the Ru-C(aryl) bond is broken *via* a proton-transfer from H_2O to the carbon atom and the hydroxyl group from H_2O migrates to the potassium cation, formally releasing KOH. Thus, a new K_2CO_3 molecule enters in the catalytic cycle serving as a ligand to ruthenium leading to intermediate **INT5**, in which the benzamide product is already coordinated to the catalyst. The theoretical evidence of the second additional K_2CO_3 molecule is in agreement with the experimental requirements of an excess of base to reach good yields of the benzamide product. The elementary step (**INT4** → **INT5**) is well supported by the experimental evidence that 1.5 equivalents of water are enough to the catalysis for completion (Table 1). Next step is supported by the excess of K_2CO_3, together with the thermodynamic stability of **INT6** (7.1 kcal/mol). Finally, **P** is released *via* **TS5** with an energy barrier of 20.7 kcal/mol, however 27.4 kcal/mol from **INT4** (Figure 1A). Experimentally, **2** is obtained from **P** by an acidic work-up.

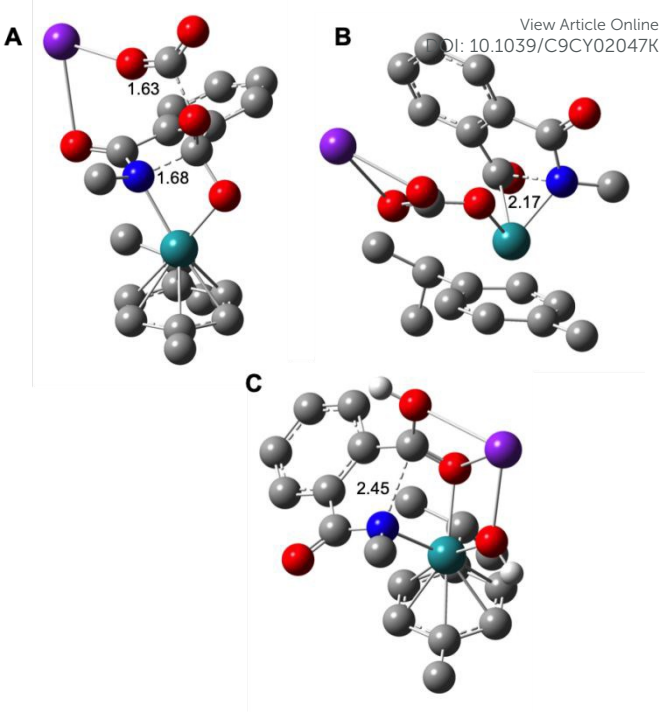

Figure 2. Computed molecular structures of the five-membered ring opening rate determining step **TS2** in the case of K_2CO_3 as a base for the assisted mechanism of Figure 1, (**A**); without considering the intramolecular nucleophilic attack from **INT1** to **INT2** (**B**); In (**C**) is reported the five-membered ring opening **TS2'** of Figure 3 for the KOH assisted mechanism. H atoms omitted for clarity (except the protic ones). Selected distances are displayed in Å. Color code: Ru in green, K in purple, O in red, N in blue and C in gray.

In the case of the product selectivity controlled by KOH, we reasoned that the catalytically active ruthenium species might be the mononuclear $[Ru(OH)_2(p\text{-cymene})K]^+$ complex (**CAT'**, Figure 1B) similar to the experimental findings from Stephenson and co-workers.[20] For that, the calculations performed for the reaction of $[RuCl_2(p\text{-cymene})]_2$ with KOH forming **CAT'** and KCl led to a highly favourable exergonic process with ΔG = -55.6 kcal/mol (see ESI for details). In this case, we considered that four water molecules form a hydration cluster with KOH, as it was already noted elsewhere.[21,22]

Differently from the case of K_2CO_3, the substrate **1** cannot coordinate to catalyst **CAT'** according to calculations (Figure 1B). In fact, a carbonyl group of **1** directly undergoes a nucleophilic attack by an hydroxyl-coordinated to ruthenium *via* **TS1'** with an energy barrier of 26.2 kcal/mol (Figure 1B). The resulting intermediate **INT1'** presents a carbon atom that has switched its hybridization from sp^2 to sp^3 resulting in an elongation of the C-N bond of 0.17 Å (from 1.39 Å in **1** to 1.56 Å in **INT1'**). Importantly, the nucleophilic attack of the KOH base and the subsequent C-N bond elongation in **1** both together promote the five-membered ring-opening of substrate **1**.

The rate determining step for the OH^- assisted mechanism is the five-membered ring-opening of **1** (**TS2'** of Figure 1B)

analogously to the KCO_3^- assisted mechanism (**TS2** of Figure 1A); however, we calculated a lower energy barrier for **TS2'** (29.1 kcal/mol) compared with 44.0 kcal/mol of **TS2**. Such observation is a direct consequence of the longer distance of the C-N bond observed in **INT1'** ($\Delta d_{C\text{-}N}$ = 0.17 Å, Figure 1B) compared to **INT2** ($\Delta d_{C\text{-}N}$ = 0.06 Å, Figure 1A). This finding suggests a higher reactivity of the $[Ru(OH)_2(p\text{-cymene})K]^+$ complex (**CAT'**) than the $[Ru(p\text{-cymene})(\kappa^2\text{-}O_2COK)]^+$ complex (**CAT**) even at low temperatures. However, experimentally, **CAT'** does not yield any secondary amide **2** as product, but phthalamic acid derivative **3** at low temperatures (Table 1, entry 6). Indeed, the intermediate **INT2'** can be considered as the product **3** coordinated to the $[Ru(OH)(p\text{-cymene})]^+$ complex (Figure 1B).

Following an alternative mechanistic pathway (Figure 3), the addition of a KOH molecule easily releases product **P'**, the K^+ salt of **3** and regeneration of the catalyst *via* the transition state **TS3"** with an overall energetic barrier of 13.0 kcal/mol with respect to **CAT'** (Figure 3). On the other hand, the pathway leading to the formation of product **2** (Figure 1B) requires the two-fold overcoming of energetic barriers higher than 13.0 kcal/mol, which are (1) the decarboxylation of the substrate *via* **TS4'** with an energetic barrier of 20.1 kcal/mol, (2) the protonation of the ruthenium-coordinated C(aryl) atom by a water molecule *via* **TS5'** with an energetic barrier of 25.0 kcal/mol.

The results of these two competitive paths explains why at low temperature the Ru-catalysed process leads preferentially to product **3**, while by increasing the temperature all the barriers of the catalytic process are overcome, affording a selectivity toward product **2** at 150°C of the 72% (Table 1, entry 4).

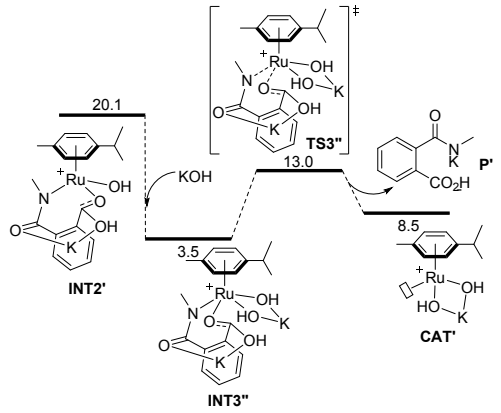

Figure 3. Computed, minimum free energy reaction profile (in kcal/mol) for the formation of phthalimic acid derivative **P'** from the ruthenium intermediate **INT2'** assisted by KOH.

Conclusions

In summary, by means of experimental and thorough theoretical calculations we have shown that the ruthenium-catalyzed protodecarbonylation of phthalimide derivatives into secondary amides proceeds under a mechanism involving release of two CO_2 molecules: one from the substrate and one from the K_2CO_3 used as reagent. Interestingly, it was found that the ruthenium center displays an oxidation state +2 through the whole catalytic cycle and the potassium cations are relevant to stabilise all the intermediates *via* weak interactions with the carbonyl groups present either in the substrate and/or the carbonate ligands. The catalysis performed in the presence of KOH as the base at high temperature led to the formation of the secondary amide product, however, at low temperature the formation of a phthalamic acid derivative was exclusively observed indicating a switch in the reaction mechanism that has been rationalized by theoretical calculations as well. Although in both cases (KOH and K_2CO_3), the rate determining step is the same, namely the five-membered ring opening of phthalimide, the presence of KOH in the reaction mixture facilitates an unexpected side-reaction towards phthalamic acid, which is not the case for K_2CO_3. Consequently, this work shows the non-trivial, multiple roles that the bases can play in reactions catalysed by ruthenium complexes and it provides insights into new mechanistic hypothesis that might be considered in related transition metal-based catalytic reactions.

Experimental section

General methods

All reagents were obtained from commercial sources and used as supplied. All reactions were carried out in flame-dried glassware under argon atmosphere unless otherwise noted. Catalytic experiments were performed in Schlenk-type flasks under argon atmosphere unless otherwise noted. Organic solutions were concentrated under reduced pressure using a rotary evaporator. Thin-layer chromatography (TLC) were carried out on 0.25 mm Merck silica gel (60-F254). Flash column chromatography was performed using silica gel Silica 60 M, 0.04-0.063 mm. *N*-Methyl-2-pyrrolidone (NMP) was distilled under reduced pressure and stored under molecular sieves and argon atmosphere. Technical grade petroleum ether (40-60) and ethyl acetate were used for column chromatography. $CDCl_3$ was stored under nitrogen over molecular sieves. NMR spectra were recorded on an AVANCE III 400 spectrometer. ^1H NMR spectra were referenced to residual protiated solvent (δ = 7.26 ppm for $CDCl_3$) and ^{13}C chemical shifts are reported relative to deuterated solvents (δ = 77.0 ppm for $CDCl_3$). The peak patterns are indicated as follows: s, singlet; d, doublet; t, triplet; q, quartet; m, multiplet, and br. for broad. GC-MS analyses were performed with a GCMS-QP2010S (Shimadzu) instrument with a GC-2010 equipped with a 30 m capillary column (Supelco, SLBTM-5ms, fused silica capillary column, 30 m x 0.25 mm x 0.25 mm film thickness), which was used with helium as the vector gas. The following GC conditions were used: initial temperature 80 °C for 2 minutes, then rate 20 °C/min until 280 °C and 280 °C for 28 minutes. HRMS were recorded on a Waters Q-Tof 2 mass spectrometer at the corresponding facilities of the CRMPO, Centre Régional de Mesures Physiques de l'Ouest, Université de Rennes 1.

Synthesis and characterization of substrate 1

Phthalimide (7 mmol, 1.03 g, 1 equiv.), potassium carbonate (14 mmol, 2.59 g, 2 equiv.) and iodomethane (14 mmol, 2 equiv.) were heated at 40 °C in *N*,*N*-dimethylformamide (6 mL) for 18 hours. After solvents evaporation under vacuum, water was added to the reaction mixture followed by extraction with DCM. The combined organic phases were dried over $MgSO_4$, filtered, and concentrated in vacuo. The desired phthalimide **1** was purified by silica gel column chromatography with a mixture of petroleum ether and ethyl acetate as eluent in 88% isolated yield. *N*-Methylphthalimide (**1**): ^{1}H NMR (400 MHz, $CDCl_3$): δ = 7.78 (dd, *J* = 5.6 Hz, 3.2 Hz, 2H), 7.66 (dd, *J* = 5.6 Hz, 3.2 Hz, 2H), 3.13 (s, 3H) ppm. The spectral data match those previously reported.[23]

General procedure for the catalysis and characterization of 2-3

$[RuCl_2(p\text{-cymene})]_2$ (0.004 mmol, 2.5 mg, 0.01 equiv.), base (1.2 mmol, 165.8 mg, 3 equiv.), distilled water (0.6 mmol, 10.8 mg, 10.8 μL, 1.5 equiv.), substrate **1** (0.4 mmol, 1 equiv.) and *N*-methyl-2-pyrrolidone (2.0 mL) were introduced in a flame-dried Schlenk tube under argon atmosphere. The reaction mixture was stirred at 150 °C during 6 hours. Then, the reaction mixture was cooled down to room temperature and diluted with water (20 mL). Then, HCl (1 M) was added until pH reached *ca.* 7. The aqueous phase was extracted with ethyl acetate (3 x 20 mL) and the combined organic layer was dried over anhydrous $MgSO_4$, filtered, and concentrated in vacuo. After solvents evaporation, the crude product **2** was obtained. [Note: In order to detect product **3** a small change in the work-up was performed using excess of HCl in order to reach pH *ca.* 1.]

***N*-Methylbenzamide (2):** Isolated by column chromatography (SiO_2, petroleum ether/ethyl acetate, 5:1 to 2:1, *v*/*v*) in 93% yield (50.3 mg) as a colourless solid. ^{1}H NMR (400 MHz, $CDCl_3$): δ = 7.77-7.74 (m, 2H), 7.49-7.45 (m, 1H), 7.42-7.38 (m, 2H), 6.42 (br. s, 1H), 2.98 (d, *J* = 4.8 Hz, 3H) ppm. ^{13}C{^{1}H} NMR (100 MHz, $CDCl_3$): δ = 168.3, 134.5, 131.2, 128.3, 126.8, 26.7 ppm. GC: t_R = 8.7 min; MS (EI): *m/z* = 134 (M^+, 48), 105 (100), 77 (91), 51 (34). The spectral data match those previously reported.[24]

2-(Methylcarbamoyl)benzoic acid (3): Crude product. ^{1}H NMR (400 MHz, $CDCl_3$): δ = 7.98 (d, *J* = 7.2 Hz, 1H), 7.48-7.43 (m, 3H), 6.89 (br. s, 1H), 2.94 (d, *J* = 4.4 Hz, 3H) ppm. ^{13}C{^{1}H} NMR (100 MHz, $CDCl_3$): δ = 175.5, 171.4, 136.1, 134.0, 131.9, 125.8, 123.2, 27.1 ppm. HRMS (ESI) calcd. for $[M + Na]^+$ $C_9H_9NO_3Na$ 202.0475, found 202.0476 (1 ppm).

Computational details

All the DFT static calculations were performed with the Gausian09 set of programs,[25] using the BP86 functional of Becke and Perdew,[26-28] together with the Grimme D3 correction term to the electronic energy.[29] The electronic configuration of the molecular systems was described with the double-ζ basis set with polarization of Ahlrichs for main-group atoms (SVP keyword in Gaussian),[30] whereas for ruthenium the small−core quasi−relativistic Stuttgart/Dresden effective core potential, with an associated valence basis set (standard SDD keywords in Gaussian09) were employed.[31-33] The geometry optimizations were performed without symmetry constraints, with analytical frequency calculations for the characterization of the located stationary points. These frequencies were used to calculate unscaled zero-point energies (ZPEs) as well as thermal corrections and entropy effects at 298.15 K. Energies were obtained by single-point calculations on the optimized geometries with the M06 functional[34] and the cc-pVTZ basis set.[35] The reported free energies in this work include energies obtained at the M06/cc-pVTZ~sdd level of theory corrected with zero-point energies, thermal corrections and entropy effects evaluated at 298.15 K, achieved at the BP86-D3/SVP~sdd level plus a solvation contribute evaluated by means of PCM model (n,n-dimethylacetamide).[36]

Conflicts of interest

There are no conflicts to declare.

Acknowledgements

A.P. is a Serra Húnter Fellow, and thanks the Ministerio de Ciencia e Innovación (MICINN) of Spain for the project PGC2018-097722-B-I00, and EU for a FEDER fund (UNGI08-4E-003). Y.-C.Y., C.B. and R.G.-D. acknowledge the CNRS, Universite de Rennes 1, Rennes Metropole, China Scholarship Council (PhD grant to Y.-C.Y.), Agence Nationale de la Recherche (ANR-JCJC) and COST Action CA15106 (CHAOS) for financial support.

Notes and references

1 (*a*) R. Noyori, *Nat. Chem.,* 2009, **1**, 5-6; *(b)* L. Falivene, Z. Cao, A. Petta, L. Serra, A. Poater, R. Oliva, V. Scarano and L. Cavallo, *Nat. Chem.*, 2019, **11**, 872-879.

2 (*a*) K. Sanderson, *Nature,* 2011, **469**, 18-20; (*b*) R. A. Sheldon, *Chem. Soc. Rev.,* 2012, **41**, 1437-1451; (*c*) G. Rothenberg, *Catalysis: Concepts and Green Applications*, Wiley-VCH, Weinheim, 2008; (*d*) M. Beller, *Chem. Soc. Rev.,* 2011, **40**, 4891-4892; (*d*) R. Franke, D. Selen and A. Borner, *Chem. Rev.,* 2012, **112**, 5675-5732.

3 (*a*) S. E. Livingstone, *The Chemistry of Ruthenium, Rhodium, Palladium, Osmium, Iridium and Platinum*, Pergamon Texts in Inorganic Chemistry, Elsevier, 1973; (*b*) J. F. Hartwig, *Organotransition Metal Chemistry: From Bonding to Catalysis*, University Science Books, Sausalito, 2009; (*c*) M. Beller and C. Bolm, *Transition Metals for Organic Synthesis*, Wiley-VCH, Weinheim, 2004; (*d*) A. de Meijere and F. Diederich, *Metal-Catalyzed Cross-Coupling Reactions*, 2nd ed., Wiley-VCH, Weinheim, 2004; (*e*) A. de Meijere, S. Braese and M. Oestreich, *Metal-Catalyzed Cross-Coupling Reactions and More*, Wiley-VCH, Weinheim, 2014.

4 (*a*) E. A. Seddon and K. R. Seddon, *The Chemistry of Ruthenium*, Elsevier Science, 1984; (*b*) S.-I. Murahashi, *Ruthenium in Organic Synthesis*, Wiley-VCH, Weinheim, Germany 2004; (*c*) C. Bruneau and P. H. Dixneuf, *Ruthenium in Catalysis*, *Top. Organomet. Chem.*, **48**, Springer-Verlag, Berlin-Heidelberg, Germany 2014.

5 (*a*) R. Noyori and S. Hashiguchi, *Acc. Chem. Res.,* 1997, **30**, 97-102; (*b*) R. Noyori and T. Okhuma, *Angew. Chem. Int. Ed.*, 2001, **40**, 40-73.

6 (*a*) T. M. Trnka and R. H. Grubbs, *Acc. Chem. Res.*, 2001, **34**, 18; (*b*) R. H. Grubbs, *Tetrahedron*, 2004, **60**, 7117-7140; *(c)* R. Credendino, A. Poater, F. Ragone and L. Cavallo, *Catal. Sci. Technol.*, 2011, **1**, 1287-1297; *(d)* A. Poater and L. Cavallo, *Beilstein J. Org. Chem.*, 2015, **11**, 1767-1780.
7 S. Murai, F. Kakiuchi, S. Sekine, Y. Tanaka, A. Kamatani, M. Sonoda and N. Chatani, *Nature*, 1993, **366**, 529-531.
8 Y.-C. Yuan, R. Kamaraj, C. Bruneau, T. Labasque, T. Roisnel and R. Gramage-Doria, *Org. Lett.*, 2017, **19**, 6404-6407.
9 *(a)* Y.-C. Yuan, C. Bruneau, V. Dorcet, T. Roisnel and R. Gramage-Doria, *J. Org. Chem.*, 2019, **84**, 1898-1907; *(b)* A. Poater, S. V. C. Vummaleti and L. Cavallo, *Organometallics*, 2013, **32**, 6330-6336.
10 (*a*) S. Inoue, H. Shiota, Y. Fukumoto and N. Chatani, *J. Am. Chem. Soc.*, 2009, **131**, 6898-6899; (*b*) N. Hasegawa, V. Charra, S. Inoue, Y. Fukumoto and N. Chatani, *J. Am. Chem. Soc.*, 2011, **133**, 8070-8073.
11 Y. Du, T. K. Hyster and T. Rovis, *Chem. Commun.*, 2011, **47**, 12074-12076.
12 (*a*) L. Huang, A. Biafora, G. Zhang, V. Bragoni and L. J. Goossen, *Angew. Chem. Int. Ed.*, 2016, **55**, 6933-6937; (*b*) J. Zhang, R. Shrestha, J. F. Hartwig and P. Zhao, *Nature Chem.*, 2016, **8**, 1144-1151; (*c*) J.-L. Yu, S.-Q. Zhang and X. Hong, *J. Am. Chem. Soc.*, 2017, **139**, 7224-7243; (*d*) A. Mandal, H. Sahoo, S. Dana and M. Baidya, *Org. Lett.*, 2017, **19**, 4138-4141; (*e*) F. Pu, Z.-W. Liu, L.-Y. Zhang, J. Fan and X.-Y. Shi, *ChemCatChem*, 2019, **11**, 4116-4122.
13 T. Shiba, T. Kurahashi and S. Matsubara, *J. Am. Chem. Soc.*, 2013, **135**, 13636-13639.
14 *(a)* P. K. Samanta and P. Biswas, *J. Org. Chem.*, 2019, **84**, 3968-3976; *(b)* T.-L. Zhou, G.-C. Li, S. P. Nolan and M. Szostak, *Org. Lett.* 2019, **21**, 3304-3309. *(c)* S.-M. Wang, C. Zhao, X. Zhang and H.-L. Qin, *Org. Biomol. Chem.*, 2019, **17**, 4087-4101.
15 (*a*) P. B. Arockiam, C. Bruneau and P. H. Dixneuf, *Chem. Rev.*, 2012, **112**, 5879-5883; (*b*) L. Ackermann, *Chem. Rev.*, 2011, **111**, 1315-1345.
16 M. Simonetti, G. J. P. Perry, X. C. Cambeiro, F. Julia-Hernandez, J. N. Arokianathar and I. Larrosa, *J. Am. Chem. Soc.*, 2016, **138**, 3596-3606.
17 (*a*) S. K. Hasan and S. A. Abbas, *Can. J. Chem.*, 1975, **53**, 2450-2453; (*b*) P. P. Kumar, B. R. Devi, P. K. Dubey and S. M. G. Mohiuddin, *Green Chem. Lett. Rev.*, 2011, **4**, 341-348.
18 Y.-Y. Meng, X.-J. Si, Y.-Y. Song, H.-M. Zhou and F. Xu, *Chem. Commun.*, 2019, **55**, 9507-9510.
19 B. Demerseman, M. D. Mbaye, D. Sémeril, L. Toupet, C. Bruneau and P. H. Dixneuf, *Eur. J. Inorg. Chem.*, 2006, 1174-1181.
20 T. Arthur, D. R. Robertson, D. A. Tocher and T. A. Stephenson, *J. Organomet. Chem.*, 1981, **208**, 389-400.
21 A. Kumar, M. Park, J. Y. Huh, H. M. Lee and K. S. Kim, *J. Phys. Chem. A*, 2006, **110**, 12484-12493
22 J. Mahler and I. Persson, *Inorg. Chem.*, 2012, **51**, 425-438.
23 S. Takebayashi, J. M. John and S. H. Bergens, *J. Am. Chem. Soc.*, 2010, **132**, 12832-12834.
24 A. B. Charette, M. Grenon, A. Lemire, M. Pourashraf and J. Martel, *J. Am. Chem. Soc.*, 2001, **123**, 11829-11830.
25 M. J. Frisch, G. W. Trucks, H. B. Schlegel, G. E. Scuseria, M. A. Robb, J. R. Cheeseman, G. Scalmani, V. Barone, B. Mennucci, G. A. Petersson, H. Nakatsuji, M. Caricato, X. Li, H. P. Hratchian, A. F. Izmaylov, J. Bloino, G. Zheng, J. L. Sonnenberg, M. Hada, M. Ehara, K. Toyota, R. Fukuda, J. Hasegawa, M. Ishida, T. Nakajima, Y. Honda, O. Kitao, H. Nakai, T. Vreven, J. A. Montgomery Jr., J. E. Peralta, F. Ogliaro, M. Bearpark, J. J. Heyd, E. Brothers, K. N. Kudin, V. N. Staroverov, R. Kobayashi, J. Normand, K. Raghavachari, A. Rendell, J. C. Burant, S. S. Iyengar, J. Tomasi, M. Cossi, N. Rega, N. J. Millam, M. Klene, J. E, Knox, J. B. Cross, V. Bakken, C. Adamo, J. Jaramillo, R. Gomperts, R. E. Stratmann, O. Yazyev, A. J. Austin, R. Cammi, C. Pomelli, J. W. Ochterski, R. L. Martin, K. Morokuma, V. G. Zakrzewski, G. A. Voth, P. Salvador, J. J. Dannenberg, S. Dapprich, A. D. Daniels, O. Farkas, J. B. Foresman, J. V. Ortiz, J. Cioslowski and D. J. Fox, *Gaussian 09, Revision E.01*, Gaussian, Inc., Wallingford CT, 2009.
26 A. Becke, *Phys. Rev. A*, 1988, **38**, 3098-3100.
27 J. P. Perdew, *Phys. Rev. B*, 1986, **33**, 8822-8824.
28 J. P. Perdew, *Phys. Rev. B*, 1986, **34**, 7406-7406.
29 S. Grimme, J. Antony, S. Ehrlich and H. A. Krieg, *J. Chem. Phys.,* 2010, **132**, 154104.
30 S. Schäfer, H. Horn and R. Ahlrichs, *J. Chem. Phys.*, 1992, **97**, 2571-2577.
31 U. Haeusermann, M. Dolg, H. Stoll, H. Preuss, P. Schwerdtfeger and R. M. Pitzer, *Mol. Phys.*, 1993, **78**, 1211-1224.
32 W. Küchle, M. Dolg, H. Stoll and H. Preuss, *J. Chem. Phys.*, 1994, **100**, 7535-7542.
33 T. Leininger, A. Nicklass, H. Stoll, M. Dolg and P. Schwerdtfeger, *J. Chem. Phys.*, 1996, **105**, 1052-1059.
34 Y. Zhao and D. G. Truhlar, *Theor. Chem. Acc.*, 2008, **120**, 215.
35 R. A. Kendall, T. H. Dunning Jr. and R. J. Harrison, *J. Chem. Phys.*, 1992, **96**, 6796-6806.
36 V. Barone and M. Cossi, *J. Phys. Chem. A*, **1998**, *102*, 1995-2001.

View Article Online
DOI: 10.1039/C9CY02047K

Mechanism of the ruthenium-catalyzed protodecarbonylation of phthalimides into benzamides elucidated by experiments and calculations: the manifold roles of the bases responsible for the control of the chemoselectivity.

TOC